Journal of World Architecture, 2025, Volume 9, Issue 3
https://ojs.bbwpublisher.com/index.php/JWA
Online ISSN: 2208-3499
Print ISSN: 2208-3480

Numerical Simulation of M-Shaped Multi-Row Pile-Supported Foundation Pit Excavation Based on ABAQUS

Meng Chen[1], Chuanteng Huang[1]*, Shuang Pu[1], Jilun Cai[1], Zuocai Li[2], Yufu Huang[1]

[1]School of Engineering, Zunyi Normal University, Zunyi, China
[2]China Railway 22nd Bureau Group Electrification Engineering Co., Ltd., Beijing 100043, China

**Author to whom correspondence should be addressed.*

Copyright: © 2025 Author(s). This is an open-access article distributed under the terms of the Creative Commons Attribution License (CC BY 4.0), permitting distribution and reproduction in any medium, provided the original work is cited.

Abstract: The M-shaped multi-row pile foundation retaining structure represents an enhanced version of conventional multi-row anti-sliding support systems. To date, the implementation of M-shaped pile configurations in foundation pit excavations has not been extensively investigated, with particularly scant research focusing on their load-bearing mechanisms and stress redistribution characteristics. Furthermore, numerical modeling methodologies for such geometrically optimized pile networks remain underdeveloped compared to practical engineering applications, creating a notable research-practice gap in geotechnical engineering. A comparative finite element analysis was systematically conducted using ABAQUS software to establish three distinct excavation support configurations: single-row cantilever retaining structures, three-row cantilever configurations, and M-shaped multi-row pile foundation systems. Subsequent numerical simulations enabled quantitative comparisons of critical performance indicators, including pile stress distribution patterns, lateral displacement profiles, and bending moment diagrams across different structural typologies. The parametric investigation revealed characteristic mechanical responses associated with each configuration, establishing corresponding mechanical principles governing the interaction between pile topology and soil-structure behavior towers. The findings of this study provide critical references for the design optimization of M-shaped multi-row pile foundation retaining systems.

Keywords: M-shaped multi-row piles; Foundation pit excavation; Numerical simulation; ABAQUS

Online publication: June 30, 2025

1. Introduction

The current urbanization rate exceeding 65% in China has escalated technical challenges in deep excavation engineering and geohazard mitigation under complex construction site conditions and geological constraints. Conventional retaining structures enhance stability through increased pile cross-sectional dimensions, yet incur construction complexities and economic inefficiencies. H-shaped and M-shaped multi-row pile configurations

have emerged as a research focus due to their cost-effectiveness and structural efficiency, while M-shaped variants particularly lack sufficient theoretical substantiation and demonstrate limited field implementation maturity.

Cai demonstrated the feasibility of single-row bored pile retaining systems through ultra-deep foundation pit engineering applications [1]. Xiong identified two distinct deformation patterns ("V"-type and "W"-type configurations) in H-shaped retaining structures [2]. Li established laboratory-scale H-pile models providing theoretical foundations for optimizing cantilever length and connecting beam dimensions [3].Li developed a three-row anti-slide pile finite element model, proposing optimal pile spacing values at rock-debris interfaces [4]. Zou employed FLAC3D simulations to analyze wedge-shaped pile behavior, revealing significant regulatory effects of wedge angles on stress distribution [5]. Zhang established H-shaped pile-soil interaction models using ABAQUS, determining 2.5 times pile diameter as the optimum inter-row spacing [6]. Wu simulated pile position impacts on slope stability, identifying 3m from slope crest as the optimal layout position [7]. Zhan conducted PLAXIS3D comparisons between parallel and staggered pile arrangements, confirming that rear-row piles bear predominant load-bearing functions [8].

Current numerical modeling practices for M-shaped multi-row pile foundations predominantly focus on individual configuration analyses, with existing studies conspicuously lacking comparative investigations against conventional pile typologies. Current simulation methodologies exhibit limitations in pile arrangement diversity, with insufficient parametric investigations addressing stiffness variations in pile elements and connecting beams. Furthermore, numerical simulation studies focusing on M-shaped multi-row pile foundation retaining systems under deep excavation scenarios demonstrate notable scarcity, while the mechanical implications of critical design parameters (e.g., pile spacing ratios and flexural rigidity coefficients) on structural stress redistribution remain insufficiently quantified.

This study systematically develops finite element models in ABAQUS to comparatively analyze three excavation support systems: single-row cantilever retaining structures, three-row cantilever configurations, and M-shaped multi-row pile foundation systems. Quantitative comparisons reveal distinct patterns in pile stress distribution, lateral displacement characteristics, and bending moment diagram configurations across different structural typologies. The established mechanical principles governing load-transfer mechanisms provide practical references for geotechnical engineering design practices.

2. Numerical simulation of foundation pit excavation based on ABAQUS

2.1. Engineering problem description

As illustrated in **Figure 1**, the foundation pit exhibits the excavation width of b × S = 2m × 20m, and the depth of $H_1 = 10m$. Three distinct retaining systems are implemented: Single-row cantilever retaining structure, Three-row cantilever retaining structure, and M-shaped retaining system.

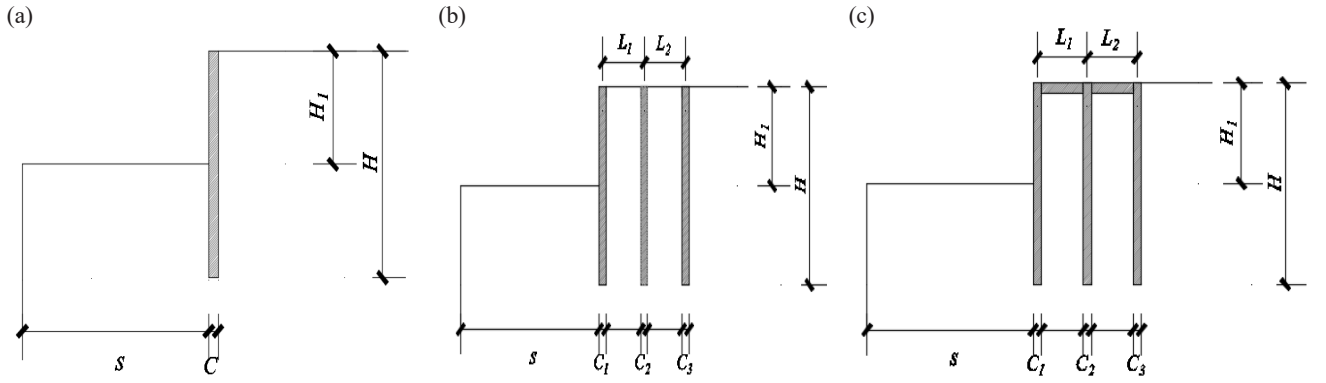

Figure 1. Diagrams of various retaining structures; (a) Cantilever retaining structure; (b) Three-row cantilever retaining structure; (c) M-shaped retaining system

All retaining piles exhibit uniform dimensions: width $C = C_1 = C_2 = C_3 = 1m$ and embedded length $H = 20m$. For multi-row configurations: Center-to-center pile spacing: $L_1 = L_2 = L_3 = 6m$; M-shaped connecting beam: Thickness $T = 1m$. Material properties are defined as: Pile elastic modulus: $E_0 = 28000000k$Pa, Soil elastic modulus: $E = 66000k$Pa, Lateral earth pressure coefficient: $K_h = 2$. The foundation pit parameters are detailed in **Table 1**, while the soil and pile properties are tabulated in **Table 2**. All connecting beam parameters exhibit identical values to those of the piles.

Table 1. Foundation pit parameters

Excavation depth H_1 (m)	Pile thickness C (m)	Pile length H (m)	Pile spacing L_0 (m)	Coupling beam thickness T (m)
10	1	20	6	1

Table 2. Pile-soil physical parameters

	Friction angle φ/(°)	Dilation angle φ'/(°)	Cohesion c/kPa	Unit weight γ/(kN·m-3)	Poisson's ratio v	Elastic modulus E (kPa)
Soil	30	0	0	20	0.2	66000
Pile	-	-	-	-	0.15	28000000

2.2. Numerical simulation of foundation pit excavation

Given the consistent modeling procedures across the three configurations, the single-row cantilever retaining structure was selected to establish the procedural framework for numerical simulation of foundation pit excavation, as detailed below:

2.2.1. Model construction and partitioning

Two-dimensional components comprising a soil domain (100 × 100 square) and pile elements (1 × 120 rectangular) were created. The geometry was partitioned to demarcate pile installation zones and excavation regions, followed by the establishment of contact interface sets.

2.2.2. Material property assignment

The Mohr-Coulomb constitutive model was assigned to the soil, while an elastic model was adopted for the piles.

Material parameters were defined as follows:

(1) Soil properties: Elastic modulus E = 66kPa, Poisson's ratio μ = 0.2, Friction angle ϕ = 30, Cohesion c = 0.1kPa

(2) Pile properties: Elastic modulus E = 28MPa, Poisson's ratio μ = 0.15

Section properties were subsequently assigned to the respective components.

2.2.3. Assembly and contact definition

Components were assembled and spatially aligned. Pile-soil contact pairs were defined with tangential behaviour governed by a penalty friction formulation (coefficient = 0.577) and normal behaviour enforcing hard contact constraints. Specific contact pairs were systematically deactivated during excavation phases to simulate progressive soil removal.

2.2.4. Analysis step configuration

Two analysis steps were established:

(1) Initial geostatic step (geo): For achieving geostatic equilibrium under gravitational loading.

(2) Excavation step (Remove): Employing asymmetric matrix storage to enhance computational convergence during contact evolution, with an increment size range of 0.1–0.2.

2.2.5. Boundary conditions and loading

Horizontal displacement constraints were imposed on the model sides, while full fixity was enforced at the base. A gravitational body force of -20 (unitless normalized acceleration) was applied to replicate geostatic loading. The initial stress field was initialized through depth-dependent stress gradients, accounting for lithostatic pressure distribution.

2.2.6. Mesh generation

A structured mesh comprising 20 × 3 incompatible modes elements was implemented. The soil domain was discretized using quadrilateral plane strain elements, with mesh density controlled through local seeding parameters (minimum element size: 0.5 units; maximum element size: 10 units).

2.2.7. Excavation simulation

Material removal in designated zones was executed via the Model Change feature, with computational tasks submitted to simulate the staged excavation process. Critical operational aspects encompassed dynamic management of contact pairs and enforcement of mesh convergence criteria.

3. Comparative analysis of different pile-type retaining structures

3.1. Numerical case design

Preliminary finite element comparative analysis of single-row, Three-row cantilever retaining structures and M-shaped pile foundation retaining structures via numerical cases are summarized in **Table 3**.

Table 3. Numerical case parameters

	Pile thickness C(m)	Pile length H(m)	Pile spacing L_0(m)	Coupling beam thickness T(m)	Elastic modulus of pile body E_0(kPa)	Elastic modulus of connecting beam E(kPa)
Cantilever retaining structure	1	20	-	-	28000000	-
Three-row cantilever retaining structure	1	20	6	-	28000000	-
M-Shaped retaining system	1	20	6	1	28000000	28000000

3.2. Analysis of results

Through finite element analysis, horizontal displacement contour maps of the retaining structures and soil mass were obtained (**Figure 2**) (Note: Positive values indicate rightward displacement, and negative values indicate leftward displacement).

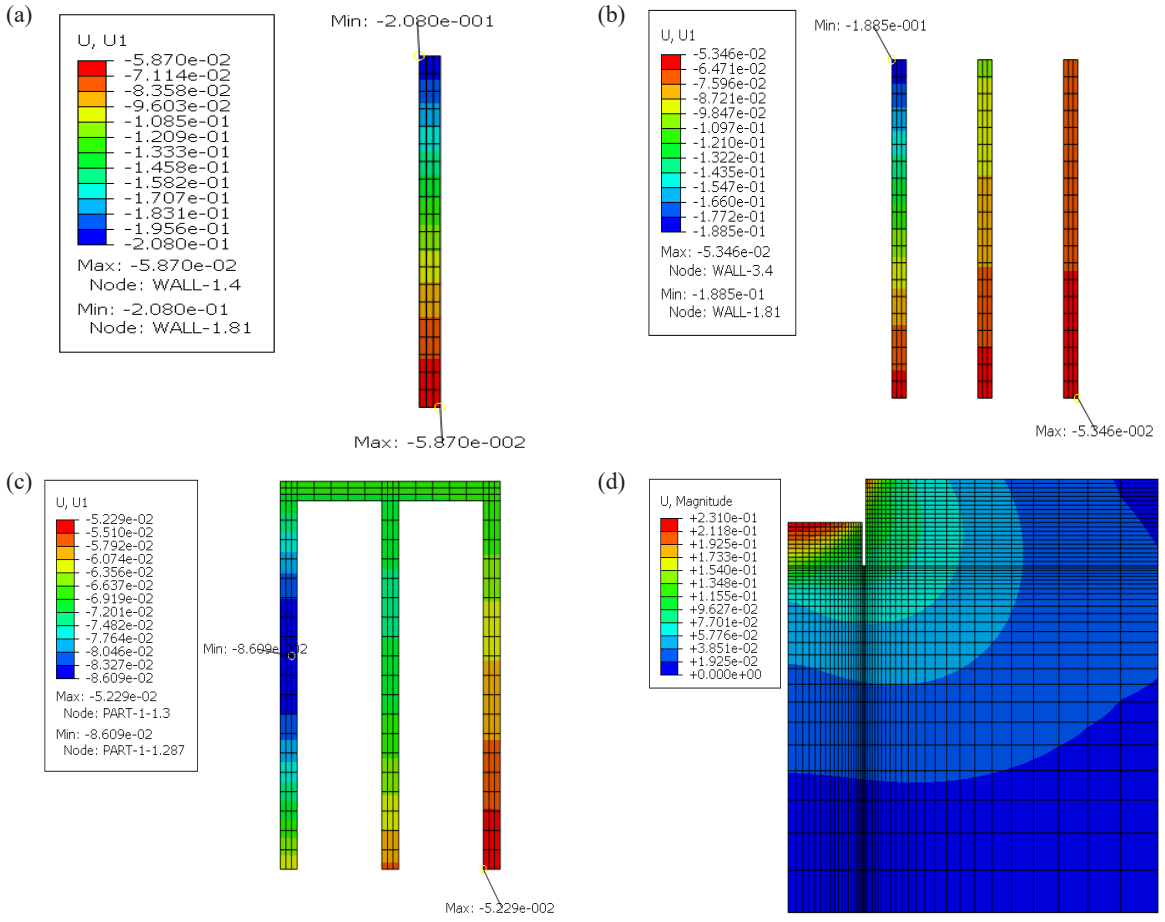

Figure 2. Horizontal displacement contour maps of various retaining structures in U1 direction; (a) Cantilever retaining structure; (b) Three-row cantilever retaining structure; (c) M-shaped retaining system; (d) Soil mass

As illustrated in **Figures 2(a)** to **2(b)**, the maximum horizontal displacements of the single-row and three-row cantilever retaining structures are located at the top, measuring 20.8 cm and 18.85 cm, respectively. The three-row cantilever system exhibits a 10.34% reduction in displacement compared to the single-row configuration.

Figure 2(c) demonstrates that the M-shaped retaining structure, owing to the constraint effect of the connecting beams, shifts the maximum displacement to 8.609 cm, representing reductions of 58.22% and 53.90% compared to the single-row and three-row cantilever systems, respectively. The study demonstrates that: The three-row cantilever system enhances safety relative to the single-row system; The M-shaped retaining structure achieves superior displacement control through the synergistic constraint mechanism of its connecting beams, significantly improving structural reliability. **Figure 3** compares the vertical (S22) stress distribution characteristics between the single-row cantilever retaining structure and the M-shaped retaining structure.

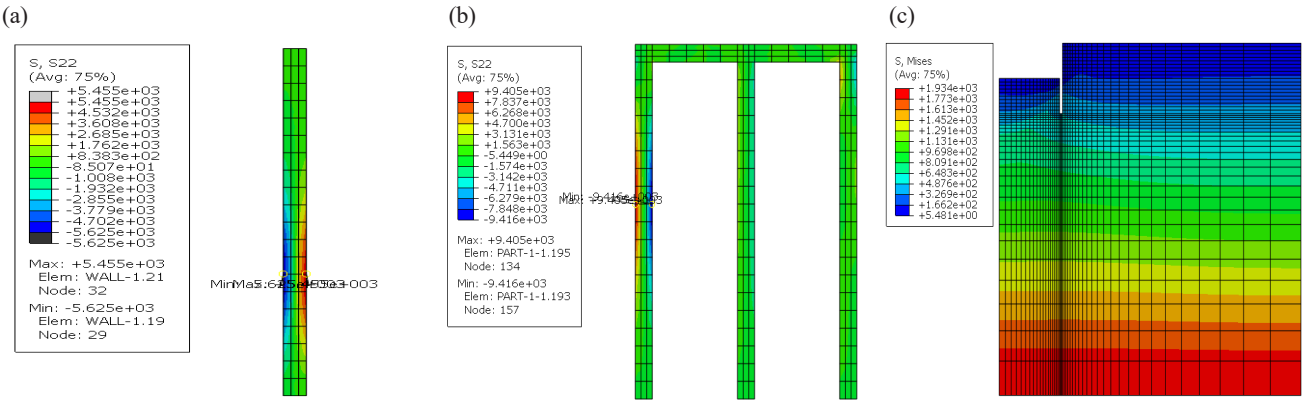

Figure 3. Stress contour maps of various retaining structures in S22 direction; (a) Cantilever retaining structure; (b) M-shaped retaining system; (c) Soil mass

3.2.1. Single-row cantilever system

Maximum compressive stress (5.625 kN) is localized on the left side of the pile body, while maximum tensile stress (5.455 kN) occurs on the right side, both concentrated in the lower two-thirds section. The bending moment diagram exhibits a positive parabolic profile, consistent with the bending behavior of a cantilever beam subjected to uniformly distributed horizontal loading.

3.2.2. M-shaped retaining structure

Owing to the synergistic constraint mechanism of the connecting beams, both maximum tensile stress (9.416 kN) and compressive stress (9.385 kN) are concentrated in the mid-section of the front-row piles. Bending moment magnitudes are significantly higher than those of the single-row system, demonstrating enhanced load redistribution capabilities.

As shown in **Figure 4**, the bending moment distribution of the M-shaped piles differs from that of the single-row configuration. The tops of the front-row piles are subjected to horizontal elastic constraints imposed by the connecting beams, while the soil squeezing effect between the piles exacerbates the bending moment magnitudes. Specifically, when the rear-row piles displace leftward, the soil between the piles is horizontally compressed and cannot heave upward (due to the vertical constraints of the connecting beams), resulting in lateral displacement of the soil near the ground surface. After excavation of the foundation pit, the lateral earth pressure on the left side of the front-row piles decreases, and the soil at the bottom rebounds upward, causing the front-row piles to bend outward due to compression from the mid-section soil. The soil squeezing effect not only disrupts the soil structure but also transmits additional loads to the pile shafts through horizontal displacement, leading to more complex stress concentration phenomena. The results indicate that although the connecting beams optimize displacement

control, the pile-soil interaction intensifies localized stress levels.

Figure 5 presents the bending moment diagrams for the three rows of piles in the M-shaped retaining structure.

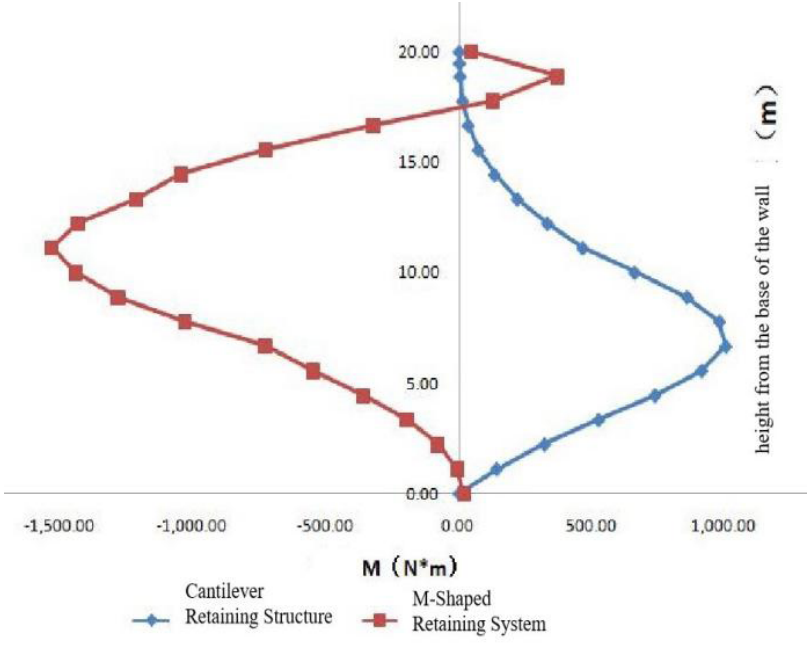

Figure 4. Bending moment diagram of front-row piles

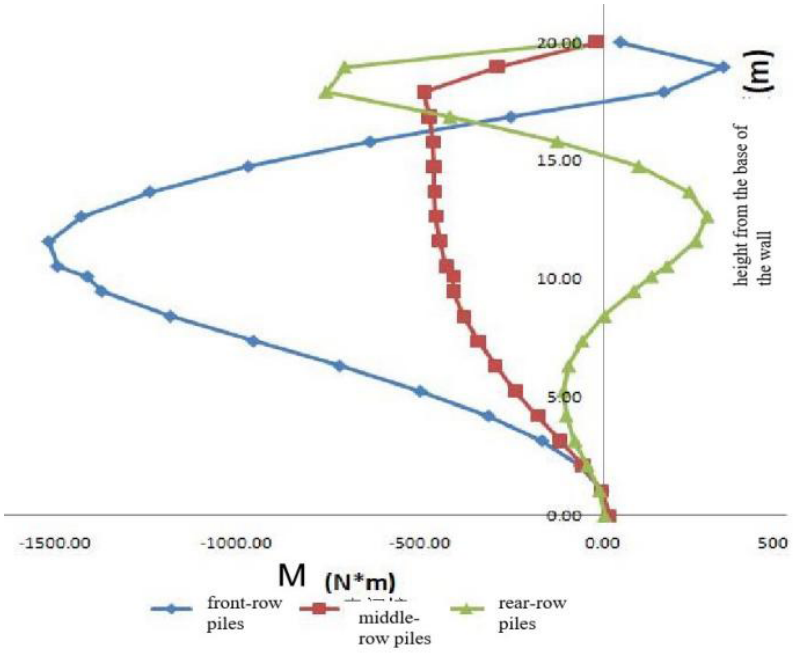

Figure 5. Bending moment diagrams for rows of piles in the m-shaped retaining structure

The maximum bending moments in the three-row pile system are located at the mid-section of the front-row piles. The middle-row piles, subjected to lateral compression from the right-side soil while simultaneously compressing the left-side soil, exhibit a relatively uniform bending moment distribution. Due to the presence of

connecting beams, which exert a horizontal tensile force toward the left on the top of the rear-row piles, negative bending moments (indicating tension on the right face) are observed in the upper one-third of these piles. The reduced soil compression on the right side of the rear-row piles compared to their left side results in positive bending moments (compression on the right face) in the mid-section of these piles.

4. Conclusion

This paper presents the modeling process of single-row cantilever retaining structures, three-row cantilever retaining structures, and M-shaped multi-row pile foundation retaining structures established using ABAQUS. The study investigates and analyzes the pile stress distribution, horizontal lateral displacement, and bending moment distribution patterns and behavioral characteristics among various retaining structures employed in foundation pit excavation.

The following conclusions are drawn from the analysis: In deep foundation pit support systems, the M-shaped retaining structure demonstrates optimal safety performance, surpassing both three-row cantilever systems and single-row cantilever systems in effectiveness. For M-shaped piles, the displacement at the pile head decreases with increasing spacing, indicating the existence of an optimal center-to-center spacing for structural stability.

In pile support systems, different structural configurations exhibit distinct bending moment behaviors. For single-row cantilever piles, the maximum bending moment typically occurs just below the excavation face, reflecting the behavior of a classic cantilever beam. In M-shaped retaining structures, the bending moment distribution varies by row. Front-row piles, modeled under fixed-pinned boundary conditions, experience their maximum bending moment above the excavation face. Middle-row piles are subject to uniform tensile stress across the cross-section on the same side, with the peak bending moment occurring at the pile head. Rear-row piles display an S-shaped bending moment distribution, characterized by a positive maximum at the pile head and a negative maximum approximately three-quarters down the pile depth.

Funding

College Students' Innovation and Entrepreneurship Training Program(Project No.: 202310664007), Science and Technology Planning Project of Zunyi City of China (Project No.: Zun Shi Ke He HZ Zi [2022] 121), Guizhou Provincial First-Class Undergraduate Major "Civil Engineering" (Project No.: Qian Jiao Han [2022] No. 61), Guizhou Provincial First-Class Course Construction Project (Project No.: 2022JKXX0165, 2024JKXN0064).

Disclosure statement

The authors declare no conflict of interest.

References

[1] Cai X, 2018, Application of Single-Row Pile Support System in Ultra-Deep Foundation Pit Support in Soft Soil Areas. Construction Technology, 40(6): 830–832+849.

[2] Xiong C, Zhang M, Chen Y, 2022, Experimental Study on H-Shaped Retaining Structures. China Civil Engineering Journal, 55(7): 108–120.

[3] Li Y, Zhang X, Zhang D, et al., 2023, Model Test Study on Mechanical Behavior of H-Shaped Anti-Slide Piles Under Curved Landslide Conditions. Engineering Mechanics, 41(7): 1–12.

[4] Li Y, Xu H, Xu Y, 2021, Influence of Pile Spacing on Mechanical Characteristics of Three-Row Anti-Slide Piles in Rock Accumulation. Subgrade Engineering, (214)1: 98–103.

[5] Zou C, He J, Wu Z, et al., 2022, Numerical Analysis of Load Transfer Mechanism for Wedge-Shaped Piles Based on FLAC3D. Geotechnical Engineering, 36(5): 739–742+759.

[6] Zhang X, 2013, Numerical Analysis of H-Shaped Anti-Slide Piles in Red Bed Landslide Treatment, thesis, University of South China.

[7] Wu M, Sheng J, Tao X, et al., 2017, Three-Dimensional Finite Element Study on the Influence of Anti-Slide Pile Positions on Slope Stability. Mining Research and Development, 37(9): 82–85.

[8] Zhan Z, Xu G, 2020, Numerical Simulation of the Influence of Different Pile Arrangements on H-Shaped Double-Row Pile Support Structures. Safety and Environmental Engineering, 27(3): 193–199.

Publisher's note

Bio-Byword Scientific Publishing remains neutral with regard to jurisdictional claims in published maps and institutional affiliations.